Available online at www.sciencedirect.com
ScienceDirect
International Journal of Solids and Structures 44 (2007) 1533–1549
INTERNATIONAL JOURNAL OF SOLIDS and STRUCTURES
www.elsevier.com/locate/ijsolstr

Formulation and solution of some plasticity problems as conic programs

K. Krabbenhøft *, A.V. Lyamin, S.W. Sloan

Geotechnical Research Group, University of Newcastle, NSW 2308, Australia

Received 5 December 2005; received in revised form 21 June 2006
Available online 1 July 2006

Abstract

The application of conic programming to some traditionally difficult plasticity problems is considered. Convenient standard forms for conic programming of both limit and incremental elastoplastic analysis are given. The types of yield criteria that can be treated by conic programming is discussed and it is shown that the three-dimensional Mohr–Coulomb criterion can be cast as a set of conic constraints, thus facilitating efficient treatment by dedicated algorithms. Finally, the performance of a number of mixed finite elements is evaluated together with a state-of-the-art second-order cone programming algorithm.

Keywords: Plasticity; Optimization; Conic programming; Interior-point; Finite elements

1. Introduction

Yield surfaces with corners can be treated in two different ways. The most common treatment, due to Koiter (1953), assumes the existence of a number of smooth surfaces, each ascribed a plastic multiplier so that the plastic strain rate is given as a the sum of the (fictitious) rates associated with each of the surfaces meeting at the corner. This methodology is applicable whenever a corner appears as the result of the intersection of a number of regular surfaces. Typical examples include cap–cone models for geomaterials and single crystal plasticity models.

Singularities of the type encountered at the apex of the Drucker–Prager cone, where only one surface can be identified, are less amenable to this treatment.

In such cases the concept of a gradient should be replaced by that of a subgradient, originally due to Moreau (1963). This concept implies that the normal to the yield surface at the singularity is nonunique, but confined to the cone formed by the normal vectors emanating from the singularity. This in effect imposes a constraint, of the same type as the yield constraint, on the plastic strain state. Using these concepts, plasticity

* Corresponding author. Tel.: +61 2 4921 5734.
E-mail address: kristian.krabbenhoft@newcastle.edu.au (K. Krabbenhøft).

0020-7683/$ - see front matter © 2006 Elsevier Ltd. All rights reserved.
doi:10.1016/j.ijsolstr.2006.06.036

theory can be formulated in a particularly rigorous and general way as demonstrated by Moreau (1976), Reddy and Martin (1994), Han and Reddy (2001), and others.

The classical numerical treatment of plasticity relies for the most part on Koiter's methodology. This is the case for the implicit methods developed by Simo (1998) and his coworkers, as well as the mathematical programming methods commonly applied to limit analysis (Krabbenhøft and Damkilde, 2003; Christiansen and Andersen, 1999; Lyamin and Sloan, 2002a,b; Zouain et al., 1993; Borges et al., 1996) – a notable exception, though, being the work of Pontes et al. (1997). Thus, the standard interior-point paradigm, e.g., (Nash and Sofer, 1996; Wright, 1997; Vanderbei, 2001), makes extensive use of Lagrange multiplier techniques and Koiter's methodology then follows naturally.

In recent years a significant amount of work has been dedicated to so-called conic programming. Here, a methodology, which in many ways is similar to the one introduced by Moreau for plasticity, is used. Indeed, when applied to plasticity this framework can be seen as a direct numerical treatment of this variant of plasticity theory. Notably, the existence of singularities does not involve any problems, in theory or in practice and, using various other concepts developed within the optimization community over the last few decades, practical algorithms applicable to realistic large-scale problems have been developed, e.g., (Sturm, 1999; Andersen et al., 2003; Tutuncu et al., 2003).

Although conic programming is relatively well-established, very few applications of it have been made in the field of plasticity. This is despite its obvious appeal for problems involving singular yield surfaces. In geomechanics such problems arise in the analysis of cohesive-frictional materials and, in particular, purely frictional materials where, in common boundary value problems such as the analysis of footings, a large number of the stress points can be expected to be located close to or at the apex of the yield surface. Of the few applications made we can mention the work of Makrodimopoulos and Martin (2005a,b) who have recently applied second-order cone programming (SOCP) to some traditionally difficulty problems with considerable success. Applications to smooth problems, where conic programming is less appealing but still applicable, have also been successful (Gilbert and Tyas, 2003; Makrodimopoulos, 2006; Bisbos et al., 2005).

In this paper some aspects of the application of conic programming to plasticity problems are investigated. Throughout we focus on the solution of practical problems without trying to derive a complete framework. First, in Section 2, some basic properties of conic programming and its relation to linear programming are discussed. This is done primarily in the setting of limit analysis and relevant conic standard forms are presented. Some of the more common types of cones are then reviewed and their applicability to the Drucker–Prager, Mohr–Coulomb and Nielsen criteria are demonstrated. The most important result here is that the three-dimensional Mohr–Coulomb criterion can be cast as a set of conic constraints. In Section 3, the application of conic programming to elastoplasticity is discussed and a convenient standard form is derived. In Section 4 some finite element discretizations are briefly covered, including 2D solid elements and a lower bound element for laterally loaded plates. In Section 5 a number of test examples, focusing on the above mentioned difficulties with sigularities, are solved using the commercial code MOSEK (partly documented in Andersen et al. (2003)). Both limit and incremental elastoplastic analysis problems are presented before conclusions are drawn in Section 6.

1.1. Linear programming

All linear programs can be expressed in the following standard form

$$\begin{aligned} &\text{minimize} && \boldsymbol{c}^{\mathrm{T}}\boldsymbol{x} \\ &\text{subject to} && \boldsymbol{A}\boldsymbol{x} = \boldsymbol{b} \\ & && \boldsymbol{x} \leqslant \boldsymbol{0} \end{aligned} \tag{1}$$

This canonical form is commonly used in the optimization literature. In the following, however, we will use a slightly different form given by

$$\begin{aligned} &\text{minimize} && \alpha \\ &\text{subject to} && \boldsymbol{B}^{\mathrm{T}}\boldsymbol{\sigma} = \alpha\boldsymbol{p} + \boldsymbol{p}_0 \\ & && \boldsymbol{\sigma} \leqslant \boldsymbol{0} \end{aligned} \tag{2}$$

Although completely general, this program can also be seen as a convenient standard form for plastic limit analysis. The scalar α is the load multiplier, $\boldsymbol{B}^{\mathrm{T}}$ the discrete equilibrium operator, and $\boldsymbol{p}$ and $\boldsymbol{p}_0$ are vectors representing variable and constant loads, respectively. The constraints $\boldsymbol{\sigma} \leqslant \boldsymbol{0}$ can be interpreted as tension cut-off yield criteria. More general yield criteria, for example of the type $\boldsymbol{F}^{\mathrm{T}}\boldsymbol{\sigma} - \boldsymbol{k} \leqslant \boldsymbol{0}$ can be included in the standard form (2) by introducing a new variable $\boldsymbol{\xi} = \boldsymbol{F}^{\mathrm{T}}\boldsymbol{\sigma} - \boldsymbol{k}$ together with the constraint $\boldsymbol{\xi} \leqslant \boldsymbol{0}$.

The dual to (2) is given by

$$\begin{aligned} &\text{minimize} && -\boldsymbol{p}_0^{\mathrm{T}}\boldsymbol{u} \\ &\text{subject to} && \boldsymbol{B}\boldsymbol{u} + \boldsymbol{e} = \boldsymbol{0} \\ & && \boldsymbol{p}^{\mathrm{T}}\boldsymbol{u} = 1 \\ & && \boldsymbol{e} \leqslant \boldsymbol{0} \end{aligned} \tag{3}$$

where, again, the physical interpretation is quite clear. Following the upper bound theorem, the internal work rate (including that due to external loads) is minimized subject to a constant external work rate and the relevant relation between the displacement rates $\boldsymbol{u}$ and the strain rates $\boldsymbol{e}$. Note, however, that by the sign convention adopted in (3), the strain rates $\boldsymbol{e}$ are of equal magnitude, but of opposite sign to the physical strain rates ε. That is, the problem (3) is equivalent to

$$\begin{aligned} &\text{minimize} && -\boldsymbol{p}_0^{\mathrm{T}}\boldsymbol{u} \\ &\text{subject to} && \boldsymbol{B}\boldsymbol{u} = \varepsilon \\ & && \boldsymbol{p}^{\mathrm{T}}\boldsymbol{u} = 1 \\ & && \varepsilon \geqslant \boldsymbol{0} \end{aligned} \tag{4}$$

from which it follows that $\boldsymbol{e} = -\varepsilon$. Although somewhat inconvenient from a mechanical point of view, the form (3) has, as will be shown, certain advantages over (4). Consider now a solution $(\alpha, \boldsymbol{\sigma})$ satisfying all constraints in (2) and a solution $(\boldsymbol{u}, \boldsymbol{e})$ satisfying all constraints in (3). The duality gap, i.e., the gap between the primal and dual objective functions is then

$$-\boldsymbol{p}_0^{\mathrm{T}}\boldsymbol{u} - \alpha = -\boldsymbol{u}^{\mathrm{T}}(\boldsymbol{B}^{\mathrm{T}}\boldsymbol{\sigma} - \alpha\boldsymbol{p}) - \alpha = -\boldsymbol{u}^{\mathrm{T}}\boldsymbol{B}^{\mathrm{T}}\boldsymbol{\sigma} = \boldsymbol{\sigma}^{\mathrm{T}}\boldsymbol{e} \geqslant 0 \Longleftrightarrow \boldsymbol{\sigma}^{\mathrm{T}}\varepsilon \leqslant 0 \tag{5}$$

In other words, if we converge through a sequence of feasible primal and dual solutions the objective functions of the two problems provide bounds to the optimal solution so that

$$\alpha < (\alpha^* = -\boldsymbol{p}_0^{\mathrm{T}}\boldsymbol{u}^*) \leqslant -\boldsymbol{p}_0^{\mathrm{T}}\boldsymbol{u} \tag{6}$$

where α^* and $\boldsymbol{u}^*$ are the solutions at the optimum when $\boldsymbol{\sigma}^{\mathrm{T}}\boldsymbol{e} = \boldsymbol{\sigma}^{\mathrm{T}}\boldsymbol{\varepsilon} = 0$. From a mechanical point of view it is interesting to note that a nonzero duality gap implies a physically unacceptable solution, i.e., one where the rate of internal work (plastic dissipation) is negative.

1.2. Conic programming

Conic programming is concerned with problems that can be cast in the standard form

$$\begin{aligned} &\text{minimize} && \boldsymbol{c}^{\mathrm{T}}\boldsymbol{x} \\ &\text{subject to} && \boldsymbol{A}\boldsymbol{x} = \boldsymbol{b} \\ & && \boldsymbol{x} \in \mathcal{K} \end{aligned} \tag{7}$$

which can be seen as a direct extension of the linear program (1). By analogy with the special linear programming form (2), we will consider the following equivalent conic programming standard form

$$\begin{aligned} &\text{minimize} && \alpha \\ &\text{subject to} && \boldsymbol{B}^{\mathrm{T}}\boldsymbol{\sigma} = \alpha\boldsymbol{p} + \boldsymbol{p}_0 \\ & && \boldsymbol{\sigma} \in \mathcal{K} \end{aligned} \tag{8}$$

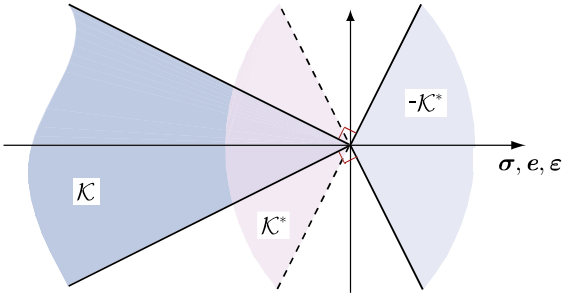

Fig. 1. Primal and dual cones.

where the conic constraint $\boldsymbol{\sigma} \in \boldsymbol{\mathcal{K}}$ is a generalization of the linear constraint $\boldsymbol{\sigma} \leqslant \mathbf{0}$. The cone $\boldsymbol{\mathcal{K}}$ can be thought of as the direct product of a arbitrary number of subcones:

$$\boldsymbol{\mathcal{K}} = \mathcal{K}_1 \times \cdots \times \mathcal{K}_N \tag{9}$$

Conic programming rests of three key assumptions about each cone $\mathcal{K}$ (Ben-Tal and Nemirovski, 2001):

$$\begin{aligned} &\mathcal{K} \text{ is closed :} && \boldsymbol{\xi}, \boldsymbol{\xi}' \in \mathcal{K} \Rightarrow \boldsymbol{\xi} + \boldsymbol{\xi}' \in \mathcal{K} \\ &\mathcal{K} \text{ is a conic set :} && \boldsymbol{\xi} \in \mathcal{K}, \lambda \geqslant 0 \Rightarrow \lambda \boldsymbol{\xi} \in \mathcal{K} \\ &\mathcal{K} \text{ is pointed :} && \mathcal{K} \cap (-\mathcal{K}) = \mathbf{0} \end{aligned} \tag{10}$$

Under these assumptions it can be shown (Ben-Tal and Nemirovski, 2001) that the dual to (8) is given by

$$\begin{aligned} &\text{minimize} && -\boldsymbol{p}_0^{\mathrm{T}} \boldsymbol{u} \\ &\text{subject to} && \boldsymbol{B}\boldsymbol{u} + \boldsymbol{e} = \mathbf{0} \\ & && \boldsymbol{p}^{\mathrm{T}} \boldsymbol{u} = 1 \\ & && \varepsilon \in \boldsymbol{\mathcal{K}}^* \end{aligned} \tag{11}$$

where the dual cone is defined by

$$\boldsymbol{\mathcal{K}}^* = \{\boldsymbol{e} \in \Re^n | \boldsymbol{\sigma}^{\mathrm{T}} \boldsymbol{e} \geqslant 0 \quad \text{for all } \boldsymbol{\sigma} \in \boldsymbol{\mathcal{K}}\} \tag{12}$$

The duality gap associated with the conic programs (8) and (11) is given by

$$-\boldsymbol{p}_0^{\mathrm{T}} \boldsymbol{u} - \alpha = -\boldsymbol{u}^{\mathrm{T}} (\boldsymbol{B}^{\mathrm{T}} \boldsymbol{\sigma} - \alpha \boldsymbol{p}) - \alpha = -\boldsymbol{u}^{\mathrm{T}} \boldsymbol{B}^{\mathrm{T}} \boldsymbol{\sigma} = \boldsymbol{\sigma}^{\mathrm{T}} \boldsymbol{e} \geqslant 0 \Longleftrightarrow \boldsymbol{\sigma}^{\mathrm{T}} \boldsymbol{\varepsilon} \leqslant 0 \tag{13}$$

where the inequalities follow from the definition of the dual cone (12) and the interpretation of the variables $\boldsymbol{e}$ as the physical strain rates ε with the sign reversed. The mechanical interpretation of the duality gap is identical to that of linear programming, i.e., the only physically acceptable solutions are ones where the plastic dissipation is equal to zero so that $\boldsymbol{\sigma}^{\mathrm{T}} \boldsymbol{e} = \boldsymbol{\sigma}^{\mathrm{T}} \boldsymbol{\varepsilon} = 0$.

From the fundamental assumptions (10), it appears that the types of constraints of interest in limit analysis must necessarily define cones with straight generators in principal stress space. Such constraints encompass, amongst others, the Mohr–Coulomb, von Mises, Hill, and Drucker–Prager yield criteria. For the purely frictional versions of these yield criteria it is easy to show that the plastic dissipation is equal to zero[1] if an associated flow rule is used and the only resistance to deformation is thus the displacement of self-weight.

The graphical interpretation of the primal and dual cones is shown in Fig. 1. It should here be noted that, in general, the cones do not need to be symmetric about a particular axis as indicated in the figure. Indeed, the criterion proposed by Nielsen (1984) is an example of a conic yield criterion which does not possess this kind of symmetry.

[1] A finite cohesion can be included by translating the cone along the hydrostatic axis. The dissipation can then be made equal to zero in a appropriately transformed stress space whereas, in physical stress space, it will be finite, see for example Section 2.1.1.

2. Specific cones

The definition of a cone is relatively broad and often non-conic constraints can be reformulated to comply with the fundamental restrictions (10). So far, however, robust algorithms have only been developed for a limited number of cones. The two most common of these are the second-order and the positive semidefinite cones.

2.1. The second-order cone

The two most common second-order cones are the quadratic cone

$$\mathcal{K}_q = \left\{ \boldsymbol{x} \in \mathfrak{R}^{m+1} | x_1 \geqslant \sqrt{\sum_{j=2}^{m+1} x_j^2} \right\} \tag{14}$$

and the rotated quadratic cone

$$\mathcal{K}_r = \left\{ \boldsymbol{x} \in \mathfrak{R}^{m+2} | 2x_1 x_2 \geqslant \sum_{j=3}^{m+2} x_j^2,\ x_1, x_2 \geqslant 0 \right\} \tag{15}$$

where it can be shown that $\mathcal{K}_r$ can be obtained from $\mathcal{K}_q$ by a linear transformation (Andersen et al., 2003). Common to these cones is that they are self-dual, or self-scaled, meaning that

$$\mathcal{K}_q = \mathcal{K}_q^* \quad \text{and} \quad \mathcal{K}_r = \mathcal{K}_r^* \tag{16}$$

Such cones occur 'naturally' in some cases, for example for a two-dimensional friction law of the type $|\tau| \leqslant c + \sigma \tan\phi$ with $c = 0$ and $\phi = 45°$. If this is not the case, see e.g., Fig. 1, a linear transformation of the stresses can be introduced to bring the problem on self-dual form. For our friction law we can introduce a new variable $\sigma' = c + \sigma \tan\phi$ so that the cone describing the constraint $|\tau| \leqslant \sigma'$ is self-dual. In the following, the self-dual conic forms of some common yield criteria are briefly presented.

2.1.1. Plane strain Mohr–Coulomb criterion

This criterion is given by

$$f(\sigma_x, \sigma_y, \tau_{xy}) = \sqrt{(\sigma_x - \sigma_y)^2 + 4\tau_{xy}^2} + (\sigma_x + \sigma_y)\sin\phi - 2c\cos\phi \leqslant 0 \tag{17}$$

where x and y refer to the in-plane directions. This constraint can be cast in terms of a conic quadratic constraint:

$$\boldsymbol{\rho} \in \mathcal{K}_q, \quad \mathcal{K}_q = \left\{ \boldsymbol{\rho} \in \mathfrak{R}^3 | \rho_1 \geqslant \sqrt{\rho_2^2 + \rho_3^2} \right\} \tag{18}$$

with the transformation between $\boldsymbol{\rho}$ and $\boldsymbol{\sigma}$ being defined by

$$\boldsymbol{\rho} = \boldsymbol{D}\boldsymbol{\sigma} + \boldsymbol{d} \tag{19}$$

where

$$\boldsymbol{D} = \begin{bmatrix} \sin\phi & \sin\phi & 0 \\ 1 & -1 & 0 \\ 0 & 0 & 2 \end{bmatrix}, \quad \boldsymbol{d} = \begin{bmatrix} 2c\cos\phi \\ 0 \\ 0 \end{bmatrix} \tag{20}$$

and $\boldsymbol{\sigma} = (\sigma_x, \sigma_y, \tau_{xy})^{\mathrm{T}}$. The transformation matrix $\boldsymbol{D}$ is here non-singular for $\phi > 0$, a fact which can be exploited when setting up the relevant limit analysis problem (see Section 3).

2.1.2. Nielsen criterion

For assessment of the ultimate load bearing capacity of two-dimensional reinforced concrete structures (plates loaded either in their own plane or subjected to lateral loading) the yield criterion proposed by Nielsen (1984) is often used. With reference to lateral loading this criterion can be written as

$$\begin{aligned} &(m_{px}^{+} - m_x)(m_{py}^{+} - m_y) \geqslant m_{xy}^2 \\ &(m_{px}^{-} + m_x)(m_{py}^{-} + m_y) \geqslant m_{xy}^2 \\ &-m_{px}^{-} \leqslant m_x \leqslant m_{px}^{+} \\ &-m_{py}^{-} \leqslant m_y \leqslant m_{py}^{+} \end{aligned} \tag{21}$$

Defining compressive (positive) bending as that resulting in compression of the top-side fibers, m_{px}^{+} and m_{py}^{+} are the compressive yield moments in the x and y directions, and similarly, m_{px}^{-} and m_{py}^{-} are the tensile yield moments in these two directions. Thus, m_{px}^{+} and m_{py}^{+} are functions of the concrete compressive strength σ_c and the bottom-side reinforcement, whereas m_{px}^{-} and m_{py}^{-} are related to σ_c and the top-side reinforcement (see Nielsen (1984) for details). Geometrically, the constraints (21) depict two intersecting cones as shown in Fig. 2. For $m_{px}^{+} = m_{py}^{-} = m_{px}^{+} = m_{py}^{-} = m_p$ the square yield criterion of Johansen (1962) is recovered. We can now define

$$\boldsymbol{D}^{+} = \frac{1}{\sqrt{2}}\begin{bmatrix} -1 & 0 & 0 \\ 0 & -1 & 0 \\ 0 & 0 & 1 \end{bmatrix}, \quad \boldsymbol{d} = \frac{1}{\sqrt{2}}\begin{pmatrix} m_{px}^{+} \\ m_{py}^{+} \\ 0 \end{pmatrix}, \quad \boldsymbol{\rho}^{+} = \begin{pmatrix} \rho_x^{+} \\ \rho_y^{+} \\ \rho_{xy}^{+} \end{pmatrix}, \tag{22}$$

and again introduce the transformation $\boldsymbol{\rho}^{+} = \boldsymbol{D}^{+}\boldsymbol{\sigma} + \boldsymbol{d}$ where $\boldsymbol{\sigma} = (m_x, m_y, m_{xy})^{\mathrm{T}}$. The first constraint of (21), together with the conditions $m_x \leqslant m_{px}^{+}$ and $m_y \leqslant m_{py}^{+}$, can then be expressed as a rotated quadratic cone according to

$$\boldsymbol{\rho} \in \mathcal{K}_r^{+}, \quad \mathcal{K}_r^{+} = \left\{ \boldsymbol{\rho}^{+} \in \Re^3 | 2\rho_x^{+}\rho_y^{+} \geqslant (\rho_{xy}^{+})^2,\ p_x^{+}, p_y^{+} \geqslant 0 \right\} \tag{23}$$

Similar expressions can be developed for the remaining constraints of (21). Again, it is seen that the transformation matrix $\boldsymbol{D}^{+}$ is invertible.

2.2. The positive semidefinite cone

The positive semidefinite cone consists of all symmetric matrices $\boldsymbol{A} \in \Re^{n\times n}$ which are positive semidefinite, i.e.,

$$\boldsymbol{x}^{\mathrm{T}}\boldsymbol{A}\boldsymbol{x} \geqslant 0 \text{ for all } \boldsymbol{x} \in \Re^n \tag{24}$$

In the following we will use the notation $\boldsymbol{A} \succeq \boldsymbol{0}$ to mean that $\boldsymbol{A}$ is positive semidefinite. Thus, a constraint of the type

$$\boldsymbol{X} \succeq \boldsymbol{0} \tag{25}$$

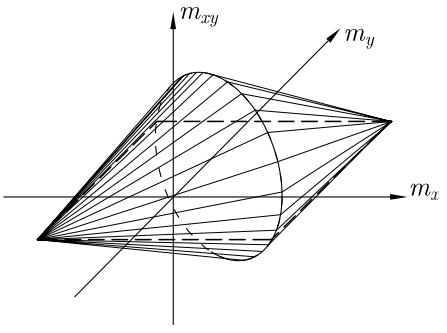

Fig. 2. Nielsen criterion.

is in fact a conic constraint. Since requiring a matrix to be positive semidefinite is equivalent to requiring that all its eigenvalues are nonnegative, this cone is of some interest in plasticity. If we consider the 3×3 symmetric stress tensor

$$\boldsymbol{\Sigma} = \begin{bmatrix} \sigma_{11} & \sigma_{12} & \sigma_{13} \\ \sigma_{12} & \sigma_{22} & \sigma_{23} \\ \sigma_{13} & \sigma_{23} & \sigma_{33} \end{bmatrix} \tag{26}$$

then the constraint

$$-\boldsymbol{\Sigma} \succeq \mathbf{0} \tag{27}$$

corresponds physically to a tension cut-off, i.e., to requiring that all principal stresses are less than or equal to zero. More interesting, however, is the fact that it is also possible to cast constraints which depend on the difference between two principal stress in the form (25). This is shown for the three-dimensional Mohr–Coulomb criterion in Appendix.

Semidefinite programs can be solved using much the same techniques as those employed for second-order cone programs, and although a number of good solvers are available, we have in this paper chosen to focus on problems that can be cast as SOCPs.

3. Limit analysis

In practice general purpose SOCP algorithms inevitably operate only on self-dual cones. Except under very special circumstances it is therefore necessary to introduce additional variables. With reference to the transformations discussed above a practical standard form of limit analysis is therefore

$$\begin{aligned} &\text{minimize} && \alpha \\ &\text{subject to} && \boldsymbol{B}^{\mathrm{T}}\boldsymbol{\sigma} = \alpha\boldsymbol{p} + \boldsymbol{p}_0 \\ &&& \boldsymbol{\rho} = \boldsymbol{D}\boldsymbol{\sigma} + \boldsymbol{d} \\ &&& \boldsymbol{\rho} \in \mathcal{K} \end{aligned} \tag{28}$$

If $\boldsymbol{D}$ is invertible this can be simplified to

$$\begin{aligned} &\text{minimize} && \alpha \\ &\text{subject to} && \boldsymbol{B}^{\mathrm{T}}\boldsymbol{D}^{-1}\boldsymbol{\rho} = \alpha\boldsymbol{p} + \boldsymbol{p}_0 + \boldsymbol{B}^{\mathrm{T}}\boldsymbol{D}^{-1}\boldsymbol{d} \\ &&& \boldsymbol{\rho} \in \mathcal{K} \end{aligned} \tag{29}$$

which contains the same number of constraints as the original problem (8), although it should be noted that $\boldsymbol{B}^{\mathrm{T}}\boldsymbol{D}^{-1}$ may be significantly more dense than the original constraint matrix $\boldsymbol{B}^{\mathrm{T}}$.

4. Incremental elastoplastic analysis

We now turn our attention to developing a convenient standard form for the problem of incremental elastoplastic analysis. In Krabbenhøft et al. (in press) three equivalent forms were derived using Lagrangian duality theory. It was then argued that the most convenient form was the maximization problem given by

$$\begin{aligned} &\text{minimize} && \alpha_{n+1} - \frac{1}{2}(\boldsymbol{\sigma}_{n+1} - \boldsymbol{\sigma}_n)^{\mathrm{T}}\boldsymbol{M}(\boldsymbol{\sigma}_{n+1} - \boldsymbol{\sigma}_n) \\ &\text{subject to} && \boldsymbol{B}^{\mathrm{T}}\boldsymbol{\sigma}_{n+1} = \alpha_{n+1}\boldsymbol{p} + \boldsymbol{p}_0 \\ &&& \boldsymbol{f}(\boldsymbol{\sigma}_{n+1}) \leqslant \mathbf{0} \end{aligned} \tag{30}$$

The subscripts n and $n+1$ here refer to the known and unknown states, respectively, and $\boldsymbol{M}$ is a matrix of elastic compliances so that $\varepsilon^{\mathrm{e}} = \boldsymbol{M}\boldsymbol{\sigma}$ where ε^{e} are the elastic strains. When solving this problem using standard

nonlinear programming methods the displacement increments and plastic multipliers appear as the Lagrange multipliers associated with the equilibrium and yield constraints, respectively.

4.1. Elasticity

The first obstacle to writing (30) in conic programming standard form is the nonlinearity of the objective function. This may be handled as follows. First, consider the purely elastic problem:

$$\begin{aligned} &\text{minimize} \quad \alpha_{n+1} - \frac{1}{2}(\boldsymbol{\sigma}_{n+1} - \boldsymbol{\sigma}_n)^{\mathrm{T}} \boldsymbol{M} (\boldsymbol{\sigma}_{n+1} - \boldsymbol{\sigma}_n) \\ &\text{subject to} \quad \boldsymbol{B}^{\mathrm{T}} \boldsymbol{\sigma}_{n+1} = \alpha_{n+1} \boldsymbol{p} + \boldsymbol{p}_0 \end{aligned} \tag{31}$$

It is straightforward to verify that this problem is equivalent to

$$\begin{aligned} &\text{minimize} \quad \alpha_{n+1} - x_{n+1} \\ &\text{subject to} \quad \boldsymbol{B}^{\mathrm{T}} \boldsymbol{\sigma}_{n+1} = \alpha_{n+1} \boldsymbol{p} + \boldsymbol{p}_0 \\ &\qquad\qquad \frac{1}{2}(\boldsymbol{\sigma}_{n+1} - \boldsymbol{\sigma}_n)^{\mathrm{T}} \boldsymbol{M} (\boldsymbol{\sigma}_{n+1} - \boldsymbol{\sigma}_n) - x_{n+1} \leqslant 0 \end{aligned} \tag{32}$$

where a new variable x_{n+1} has been introduced. At the optimum, the last restriction will be satisfied as an equality. This problem can be cast as a SOCP by introducing

$$\boldsymbol{\xi}_{n+1} = \boldsymbol{M}^{\frac{1}{2}} (\boldsymbol{\sigma}_{n+1} - \boldsymbol{\sigma}_n) \tag{33}$$

and, in addition, a scalar variable

$$y_{n+1} = 1 \tag{34}$$

The problem (32) can then be written as

$$\begin{aligned} &\text{minimize} \quad \alpha_{n+1} - x_{n+1} \\ &\text{subject to} \quad \boldsymbol{B}^{\mathrm{T}} \boldsymbol{M}^{-\frac{1}{2}} \boldsymbol{\xi}_{n+1} = \alpha_{n+1} \boldsymbol{p} + \boldsymbol{p}_0 - \boldsymbol{B}^{\mathrm{T}} \boldsymbol{\sigma}_n \\ &\qquad\qquad y_{n+1} = 1 \\ &\qquad\qquad (x, y, \boldsymbol{\xi})_{n+1} \in \mathcal{M} \end{aligned} \tag{35}$$

where $\mathcal{M}$ is a rotated quadratic cone:

$$\mathcal{M} = \left\{ (x, y, \boldsymbol{\xi}) \in \Re^{m+2} | 2xy > \boldsymbol{\xi}^{\mathrm{T}} \boldsymbol{\xi},\ x, y \geqslant 0 \right\} \tag{36}$$

The dual to this problem is given by

$$\begin{aligned} &\text{minimize} \quad -(\boldsymbol{p}_0 - \boldsymbol{B}^{\mathrm{T}} \boldsymbol{\sigma}_n)^{\mathrm{T}} \boldsymbol{v}_{n+1} - \omega_{n+1} \\ &\text{subject to} \quad \boldsymbol{M}^{-\frac{1}{2}} \boldsymbol{B} \boldsymbol{\xi}_{n+1} + \boldsymbol{e}_{n+1} = \boldsymbol{0} \\ &\qquad\qquad r_{n+1} - 1 = 0 \\ &\qquad\qquad \omega_{n+1} + t_{n+1} = 0 \\ &\qquad\qquad \boldsymbol{p}^{\mathrm{T}} \boldsymbol{v}_{n+1} = 1 \\ &\qquad\qquad (s, t, \boldsymbol{e})_{n+1} \in \mathcal{M}^* \end{aligned} \tag{37}$$

where $\boldsymbol{v}_{n+1}$, ω_{n+1}, $\boldsymbol{e}_{n+1}$, r_{n+1}, and t_{n+1} are the dual variables and

$$\mathcal{M}^* = \left\{ (r, t, \boldsymbol{e}) \in \Re^{m+2} | 2rt \geqslant \boldsymbol{e}^{\mathrm{T}} \boldsymbol{e},\ r, t \geqslant 0 \right\} \tag{38}$$

Although not immediately obvious, the constraints of (37) do in fact define the discrete elastic stress–strain–displacement relation. To see this, we first note that by virtue of the objective function ω_{n+1} will be as large as possible. Together with the conditions $r_{n+1} - 1 = 0$, $\omega_{n+1} + t_{n+1} = 0$, and $t_{n+1} \geqslant 0$ it can be verified that the condition

$$t_{n+1} = \boldsymbol{e}_{n+1}^{\mathrm{T}} \boldsymbol{e}_{n+1} \tag{39}$$

must hold at the optimum. Next, using the condition of a vanishing duality gap at the optimum we have

$$[xr + yt + \boldsymbol{\xi}^{\mathrm{T}}\boldsymbol{e}]_{n+1} = \frac{1}{2}[\boldsymbol{\xi}^{\mathrm{T}}\boldsymbol{\xi} + \boldsymbol{e}^{\mathrm{T}}\boldsymbol{e} + \boldsymbol{\xi}^{\mathrm{T}}\boldsymbol{e}]_{n+1} = \frac{1}{2}[(\boldsymbol{\xi}+\boldsymbol{e})^{\mathrm{T}}(\boldsymbol{\xi}+\boldsymbol{e})]_{n+1} = 0 \tag{40}$$

so that

$$\boldsymbol{e}_{n+1} = -\boldsymbol{\xi}_{n+1} = -\boldsymbol{M}^{\frac{1}{2}}(\boldsymbol{\sigma}_{n+1} - \boldsymbol{\sigma}_n) \tag{41}$$

Inserting this into the first constraint of (37) gives the desired relation

$$\boldsymbol{B}\boldsymbol{v}_{n+1} = \boldsymbol{M}(\boldsymbol{\sigma}_{n+1} - \boldsymbol{\sigma}_n) \tag{42}$$

where it is clear that the variables $\boldsymbol{v}_{n+1}$ should be interpreted as the displacement increments $\boldsymbol{v}_{n+1} := \boldsymbol{u}_{n+1} - \boldsymbol{u}_n$.

4.2. Elastoplasticity

It is straightforward to extend the problem (35) to include plasticity. This is done simply by limiting the stresses by the relevant yield condition so that the final elastoplastic problem reads

$$\begin{aligned}
&\text{minimize} \quad \alpha_{n+1} - x_{n+1} \\
&\text{subject to} \quad \boldsymbol{B}^{\mathrm{T}}\boldsymbol{\sigma}_{n+1} = \alpha_{n+1}\boldsymbol{p} + \boldsymbol{p}_0 \\
&\qquad\qquad \boldsymbol{\xi}_{n+1} = \boldsymbol{M}^{\frac{1}{2}}(\boldsymbol{\sigma}_{n+1} - \boldsymbol{\sigma}_n), \quad y_{n+1} = 1 \\
&\qquad\qquad (x, y, \boldsymbol{\xi})_{n+1} \in \mathcal{M} \\
&\qquad\qquad \boldsymbol{\rho}_{n+1} = \boldsymbol{D}\boldsymbol{\sigma}_{n+1} + \boldsymbol{d} \\
&\qquad\qquad \boldsymbol{\rho}_{n+1} \in \mathcal{K}
\end{aligned} \tag{43}$$

where $\mathcal{K}$ defines the yield constraints in a transformed stress space. As in the case of limit analysis the physical stresses $\boldsymbol{\sigma}$ can be eliminated to give

$$\begin{aligned}
&\text{minimize} \quad \alpha_{n+1} - x_{n+1} \\
&\text{subject to} \quad \boldsymbol{B}^{\mathrm{T}}\boldsymbol{M}^{-\frac{1}{2}}\boldsymbol{\xi}_{n+1} = \alpha_{n+1}\boldsymbol{p} + \boldsymbol{p}_0 - \boldsymbol{B}^{\mathrm{T}}\boldsymbol{\sigma}_n \\
&\qquad\qquad \boldsymbol{\rho}_{n+1} - \boldsymbol{D}\boldsymbol{M}^{-\frac{1}{2}}\boldsymbol{\xi}_{n+1} = \boldsymbol{d} + \boldsymbol{D}\boldsymbol{\sigma}_n \\
&\qquad\qquad y_{n+1} = 1 \\
&\qquad\qquad \boldsymbol{\rho}_{n+1} \in \mathcal{K}, \quad (x, y, \boldsymbol{\xi})_{n+1} \in \mathcal{M}
\end{aligned} \tag{44}$$

Note that, in contrast to what is the case with limit analysis, this reduction is always possible (as long as $\boldsymbol{M}$ is non-singular). Nevertheless, the problem (44) still contains more than twice the number of variables and equality constraints as compared to the original problem (30). Also, it should be mentioned that in practice, at least using MOSEK, the problem (43) is often faster to solve than the reduced one (44). Finally, by following the same procedure as in the purely elastic case, it can be verified that the dual to (44) gives the relevant stress–strain–displacement relation:

$$\boldsymbol{B}(\boldsymbol{u}_{n+1} - \boldsymbol{u}_n) = \boldsymbol{M}(\boldsymbol{\sigma}_{n+1} - \boldsymbol{\sigma}_n) + \Delta\varepsilon^p_{n+1}, \quad \Delta\varepsilon^p_{n+1} \in -\mathcal{K}^* \tag{45}$$

Thus, despite significant modification of the original problem (30) the Lagrange multipliers associated with the equilibrium constraints retain their physical significance as the displacement increments.

5. Finite element discretizations

5.1. Solid elements

For two-dimensional solid problems the finite element discretizations of both the limit and elastoplastic analysis problems follow that of Krabbenhøft et al. (in press) where a number of linear stress/quadratic displacement elements were discussed in some detail. If $\boldsymbol{N}_\sigma$ and $\boldsymbol{N}_u$ contain the stress and displacement interpolation functions, respectively, the quantities defining the elastoplastic analysis problem (30) are given by

$$\boldsymbol{B} = \int_{\Omega} \boldsymbol{N}_{\sigma}^{\mathrm{T}} \nabla \boldsymbol{N}_{u} \, \mathrm{d}\Omega, \quad \boldsymbol{M} = \boldsymbol{N}_{\sigma}^{\mathrm{T}} \mathbb{E}^{-1} \boldsymbol{N}_{\sigma} \, \mathrm{d}\Omega \tag{46}$$

$$\boldsymbol{p} = \int_{\Omega} \boldsymbol{N}_{u}^{\mathrm{T}} \boldsymbol{b} \, \mathrm{d}\Omega + \int_{\Gamma} \boldsymbol{N}_{u}^{\mathrm{T}} \hat{\boldsymbol{t}} \, \mathrm{d}\Gamma, \quad \boldsymbol{p}_0 = \int_{\Omega} \boldsymbol{N}_{u}^{\mathrm{T}} \boldsymbol{b}_0 \, \mathrm{d}\Omega + \int_{\Gamma} \boldsymbol{N}_{u}^{\mathrm{T}} \hat{\boldsymbol{t}}_0 \, \mathrm{d}\Gamma \tag{47}$$

where $\mathbb{E}$ is the elastic modulus and Ω and Γ are the domain and its boundary, respectively. The tractions and body forces are divided into variable parts $\hat{\boldsymbol{t}}$ and $\boldsymbol{b}$ and constant parts $\hat{\boldsymbol{t}}_0$ and $\boldsymbol{b}_0$, respectively.

By varying the numerical integration schemes for $\boldsymbol{M}$ and $\boldsymbol{B}$, a class of elements with relatively different properties can be constructed. In the following the displacements are continuous between elements and are always interpolated from the corner and midside nodes. The stresses are interpolated from three points that vary among the different elements. The matrix $\boldsymbol{M}$ is always evaluated numerically by a three-point scheme with the integration points coinciding with the stress interpolation points. Furthermore, the yield function is always enforced at these points. The force vectors $\boldsymbol{p}$ and $\boldsymbol{p}_0$ are evaluated exactly using an appropriate scheme. If all tractions and body forces are constant the standard three-point scheme is sufficient. Depending on the choice of the stress interpolation points used to evaluate the matrix $\boldsymbol{B}$, various elements may be derived. These are briefly outlined below.

5.2. Upper bound element

A rigorous upper bound element can be constructed by interpolating the stresses from the corner nodes and using these nodes as integration points for $\boldsymbol{B}$. The flow rule is then satisfied throughout the element. That is, since the displacement variation is quadratic the condition $\boldsymbol{B}\boldsymbol{u} + \boldsymbol{e} = 0$ is satisfied everywhere if it is enforced at three points, and if these three points are the corner nodes the condition $\boldsymbol{e} \in \mathcal{K}^*$ is satisfied everywhere. This element, which can be seen as a generalization of the one proposed by Yu et al. (1994), has recently been used for upper bound limit analysis of cohesive-frictional materials by Makrodimopoulos and Martin (2005a).

5.3. Displacement element I

This element uses the midside nodes as the stress interpolation and integration points. It is readily shown (Krabbenhøft et al., in press) that the standard quadratic displacement element, using the quadrature scheme with the integration points located at the midside nodes is recovered. Since the flow rule is imposed at the midside nodes it is not necessarily satisfied throughout the element and does not result in rigorously bounded limit loads (although they tend to converge from above).

5.4. Displacement element II

Same as above except that the stress interpolation and integration points are located at $(\lambda_{j-1}, \lambda_j, \lambda_{j+1}) = \left(\frac{1}{6}, \frac{4}{6}, \frac{1}{6}\right), j = 1, 2, 3$, where λ_j are the area coordinates.

5.5. Mixed element

A mixed element is constructed by using the corner nodes as the stress interpolation points and the midside nodes as the integration points. The yield condition is then satisfied throughout the element and it can be shown (Krabbenhøft et al., in press) that the limit load will always be less than or equal to that of the above three elements. It does not, however, possess any bounding properties with respect to the exact solution. This element was first proposed by Borges et al. (1996) in the context of limit analysis.

5.6. Plate element

For the limit analysis of laterally loaded plates the element proposed by Krabbenhøft and Damkilde (2002) is used. This element uses piecewise linear and discontinuous moment interpolations. If point or line loads are applied, rigorous lower bound solutions can be computed. Distributed loads are approximated by equivalent

line loads. Although this leads to solutions which are not completely rigorous lower bounds, the performance of the element is quite good and usually the limit loads converge from below.

6. Examples

In the following we solve a number of limit and elastoplastic analysis problems. In all examples the general purpose solver MOSEK is used. Default settings were used with the exception that the presolve option was suppressed (this routine eliminates redundant constraints which is not relevant for the problems considered here).

6.1. Limit analysis: strip footing on a purely frictional soil

The first example concerns the limit analysis of a smooth strip footing on a purely frictional soil obeying the Mohr–Coulomb criterion. For this problem the limit load is usually written in the form

$$V_u/B = \frac{1}{2}\gamma B N_\gamma \tag{48}$$

where γ is the soil unit weight and N_γ is the dimensionless bearing capacity factor to be determined. This problem is known to be particularly challenging, both due to the singularity at the apex of the Mohr–Coulomb cone and due to the large number of elements that typically have to be used in order to produce satisfactory results. Recently, Martin (2005) has solved the problem using the method of characteristics and obtained results which, for all practical purposes, are exact.

In the following the performance of the four elements introduced above is examined. Three different unstructured meshes, graded as indicated in Fig. 3, were used. The results of the analyses in terms of the limit loads and their deviation from Martin's results are given in Tables 1–4 for friction angles of 20°, 30°, 35°, and 40°.

The results reveal that the performance of the upper bound element is quite poor. The two displacement elements offer some improvement, but the mixed element is far superior for all meshes and all friction angles. Although somewhat surprising in view of the relatively small difference between the various elements, this trend confirms the one observed in Krabbenhøft et al. (in press) for other types of problems.

The performance of the conic optimizer was largely unaffected by the friction angle. The time required to converge was ~1 s, ~6 s, and ~50 s for the three different meshes and in all cases the number of iterations varied between 20 and 35, typically increasing with the mesh density. It should be mentioned that in some cases MOSEK terminated the iterations ("due to slow progress") before the default tolerance was reached. In all such cases, however, solutions with acceptable tolerances (typically of the order 10^{-5}–10^{-4}) were still obtained.

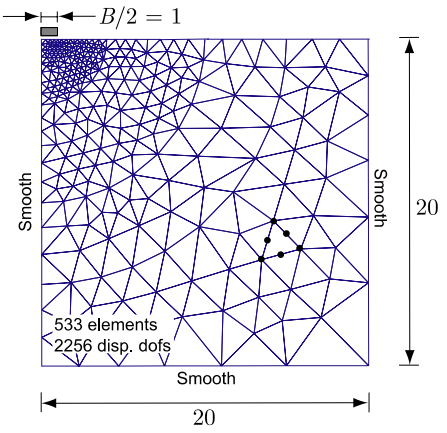

Fig. 3. Strip footing problem (coarse mesh).

Table 1
Solution statistics for smooth N_γ problem with $\phi = 20°$, $\gamma = 1$

DOFs	Upper bound elem.		Disp. elem. I		Disp. elem. II		Mixed elem.	
	N_γ	Err. (%)	N_γ	Err. (%)	N_γ	Err. (%)	N_γ	Err. (%)
2256	2.2585	+43.1	1.9646	+24.5	1.9312	+22.3	1.7085	+8.23
7976	1.9089	+20.9	1.7915	+13.5	1.7585	+11.4	1.6132	+2.19
31,176	1.7820	+12.9	1.7064	+8.09	1.6925	+7.21	1.6345	+3.54

Table 2
Solution statistics for smooth N_γ problem with $\phi = 30°$, $\gamma = 1$

DOFs	Upper bound elem.		Disp. elem. I		Disp. elem. II		Mixed elem.	
	N_γ	Err. (%)	N_γ	Err. (%)	N_γ	Err. (%)	N_γ	Err. (%)
2256	10.984	+43.5	9.3790	+22.6	8.9532	+17.0	7.7680	+1.50
7976	9.2393	+20.7	8.5554	+11.8	8.3317	+8.87	7.5196	−1.74
31,176	8.5188	+11.3	8.1660	+6.70	8.0525	+5.22	7.7414	+1.16

Table 3
Solution statistics for smooth N_γ problem with $\phi = 35°$, $\gamma = 1$

DOFs	Upper bound elem.		Disp. elem. I		Disp. elem. II		Mixed elem.	
	N_γ	Err. (%)	N_γ	Err. (%)	N_γ	Err. (%)	N_γ	Err. (%)
2256	25.449	+44.8	21.512	+22.4	20.313	+15.57	17.178	−2.27
7976	21.537	+22.5	19.666	+11.9	19.046	+8.36	17.046	−3.02
31,176	19.549	+11.2	18.699	+6.39	18.418	+4.78	17.573	−0.026

Table 4
Solution statistics for smooth N_γ problem with $\phi = 40°$, $\gamma = 1$

DOFs	Upper bound elem.		Disp. elem. I		Disp. elem. II		Mixed elem.	
	N_γ	Err. (%)	N_γ	Err. (%)	N_γ	Err. (%)	N_γ	Err. (%)
2256	63.389	+46.8	52.957	+22.6	49.845	+15.42	40.030	−7.31
7976	54.304	+25.7	48.769	+12.9	46.799	+8.36	42.202	−4.60
31,176	48.001	+11.1	45.828	+6.02	45.181	+4.62	42.703	−1.12

6.2. Elastoplastic analysis: strip footing on a purely frictional soil

Next, an elastoplastic analysis of the same problem is performed. The material parameters are the following. Young's modulus: $E = 40$ MPa, Poison's ratio: $v = 0.3$, unit weight: $\gamma = 18$ kN/m^3, cohesion: $c = 0$, and friction angle $\phi = 30°$. The state of deformation is plane and yielding is governed by the plane strain Mohr–Coulomb criterion (17). Thus, all strains, both elastic and plastic, are suppressed in the out-of-plane direction. The footing is considered rough, giving an exact bearing capacity of $V_u = 265.58$ kN (Martin, 2005). The self-weight is first applied and the analysis then proceeds by way of 25 displacement increments of equal magnitude $\Delta u = 0.4$ cm, giving a total footing displacement of 10 cm. The load–displacement curves for each of the three meshes and four elements types are shown in Fig. 4. Again, the outstanding performance of the mixed element is evident, with very little difference between the curves for the three different meshes. Regarding solutions times, a comparison between these and the ones obtained for the corresponding limit analysis problems is shown in Table 5. A steep increase in relative CPU time is seen. For standard nonlinear interior-point solvers the cost of each iteration is roughly the same regardless of whether the problem is one of limit or incremental elastoplastic analysis (Krabbenhøft and Damkilde, 2003; Krabbenhøft et al., in press). Thus, the bulk of the cpu time is spent on solving a set of linear equations of the type $\boldsymbol{K}\Delta\boldsymbol{u} = \boldsymbol{r}$ where $\boldsymbol{K}$ is of the same size and spar-

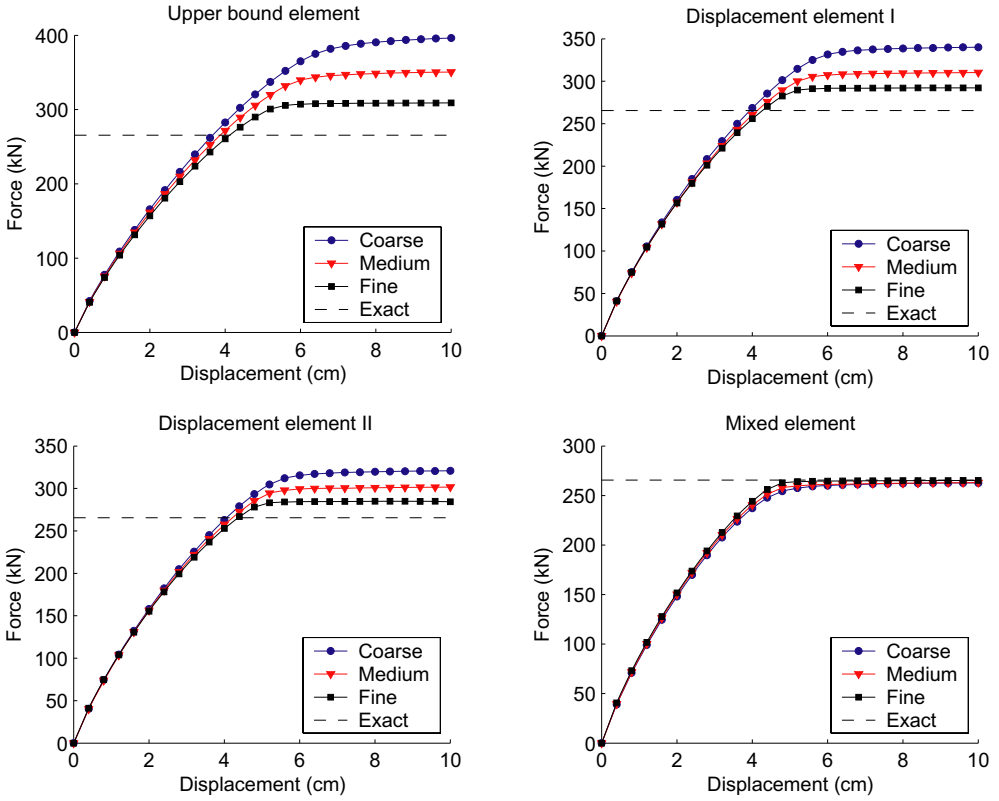

Fig. 4. Load–displacement curves for rough N_γ problem with different elements. Coarse, medium and fines meshes contain 2256, 7976, and 31,176 displacement degrees-of-freedom, respectively.

Table 5
Solution statistics for rough N_γ problem using the mixed element

Dofs	Limit analysis			Elastoplasticity[a]		
	No. iter.	t (s)	t/iter. (s)	No. iter.	t (s)	t/iter. (s)
2256	25	1.3	0.052	30	3.0	0.10
7976	24	4.4	0.18	29	15.1	0.52
31,176	27	26.4	0.98	35	115.2[b]	2.6

[a] Iteration counts and cpu times for a representative load step (averaged over a total of 25 steps).
[b] Time spent on iterations only – in addition ~75 s is spent on "matrix reordering" at the beginning of each load step before the iterations commence.

sity as a usual elastic stiffness matrix. For the conic programming standard form (44) matters are somewhat different as the elastoplastic problem contains significantly more linear constraints than the limit analysis problem. Also, the additional conic constraint accounting for elasticity could be problematic. If handled properly, however, there is little doubt that the solution time could be reduced. For example, whether the block-diagonal structure of the elasticity matrix $\boldsymbol{M}$ is exploited or not is unclear, but if not this could probably explain the dramatic increase in CPU time as compared to the corresponding limit analysis problems.

6.3. Limit analysis: reinforced concrete plate

A classical test example in the limit analysis of reinforced concrete structures is the square, clamped plate subjected to a uniform pressure. For an isotropic reinforcement layout the exact solution was found by Fox (1974) as

$$p = 42.851\, m_p/l^2 \tag{49}$$

Two different meshes as shown in Fig. 5 were used. In Table 6 the limit loads computed by means of the quasi lower bound element discussed previously are shown. As seen, the results are quite satisfactory and the performance of MOSEK was in this case somewhat better than for the Mohr–Coulomb problems, i.e., there were fewer reports of termination due to slow progress.

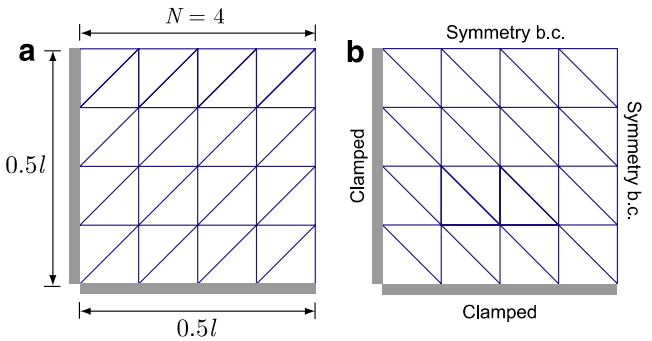

Fig. 5. Square slab subjected to uniform pressure.

Table 6
Square clamped plate: solution statistics, $l = 1.0$, $m_p - 1.0$

N	Mesh (a)				Mesh (b)			
	p	Err. (%)	Iter.	t (s)	p	Err. (%)	Iter.	t (s)
2	40.696	−5.0	10	<1	41.326	−3.6	10	<1
4	42.156	−1.6	13	<1	41.970	−2.1	13	<1
8	42.566	−0.67	18	<1	42.517	−0.78	19	<1
16	42.729	−0.29	23	2	42.729	−0.29	22	2
32	42.792	−0.14	32	12	42.800	−0.12	35	12
64	42.828	−0.054	29	61	42.831	−0.037	35	56

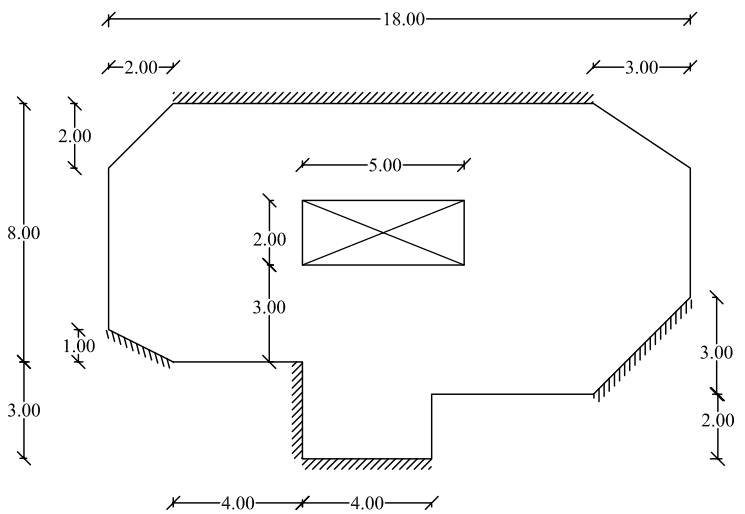

Fig. 6. Reinforced concrete plate with opening, all measurements in m.

Table 7
Optimal yield moments (kN m/m) for reinforced concrete plate with hole subjected to uniform pressure of $p = 6.75\ \mathrm{kN/m^2}$

	m_{px}^{+}	m_{py}^{+}	m_{px}^{-}	m_{py}^{-}	Mean
Isotropic	50.00	50.00	50.00	50.00	50.00
Colberg (1998)	27.83	78.65	14.56	3.26	31.08
Krabbenhøft and Damkilde (2002)	34.00	75.24	11.19	1.64	30.52
Present	31.54	76.51	7.52	0.47	29.01

6.4. Limit design: reinforced concrete plate

As a final example the limit design of the plate shown in Fig. 6 is considered. The task is to determine the optimal values of the four yield moments subject to a load bearing capacity of 6.75 $\mathrm{kN/m^2}$. This problem has previously been considered by Colberg (1998) and Krabbenhøft and Damkilde (2002). Using a mesh containing 240 elements (5040 stress and design variables) we improve slightly on the results obtained by Krabbenhøft and Damkilde (2002), see Table 7. The solution time for this problem was less than 2 s in the course of 17 iterations. The same problem, now containing 540 elements (11300 stress and design variables) was then attempted. Quite inexplicably, the solution time then increased to 150 s *per iteration* and the iterations were terminated before convergence.

7. Conclusions

Some problems of limit and incremental elastoplastic analysis have been formulated as conic programs. These include second-order as well as semidefinite programs. In the former case the solution of the problems of achieved by use of the commercial solver Mosek. Although the performance of this solver on average is quite satisfactory there were also several problematic issues as highlighted throughout the Section 5. Nevertheless, the results are encouraging and there is little doubt that a conic programming algorithm dedicated to continuum mechanical applications could be very successful. Finally, the formulation of the three-dimensional Mohr–Coulomb criterion as a set of conic (semidefinite) constraints is most interesting as this difficult yield criterion is handled in a less than ideal way using general nonlinear programming methods. However, the performance of suitable conic programming algorithms for solving this problem still remain to be evaluated.

Appendix. The 3D Mohr–Coulomb criterion as a set of semidefinite constraints

The Mohr–Coulomb criterion is given by

$$\sigma_1 - a\sigma_3 \leqslant k \tag{50}$$

where

$$a = \frac{1-\sin\phi}{1+\sin\phi}, \quad k = \frac{2c\cos\phi}{1+\sin\phi} \tag{51}$$

Here c is the cohesion, ϕ is the friction angle and $\sigma_1 \geqslant \sigma_2 \geqslant \sigma_3$ are the principal stresses, i.e., the eigenvalues of the 3×3 symmetric stress tensor $\boldsymbol{\Sigma}$. The criterion (50) can be cast as two semidefinite constraints given by

$$\boldsymbol{\Sigma} + \zeta \boldsymbol{I} \succeq \boldsymbol{0} \tag{52}$$

$$-\boldsymbol{\Sigma} + (k - a\zeta)\boldsymbol{I} \succeq 0 \tag{53}$$

where ζ is an auxiliary variable.

To demonstrate the equivalence between (50) and (52)–(53) the following well-known relations, see e.g., Golub and van Loan (1996), are useful. Let λ_j, $j = 1,\ldots,n$ be the eigenvalues of the matrix $\boldsymbol{A} \in \Re^{n\times n}$ and let $\eta \in \Re$. It can then be shown that

- The eigenvalues of $\boldsymbol{B} = \boldsymbol{A} + \eta\boldsymbol{I}$ are $\hat{\lambda}_j = \lambda_j + \eta, j = 1,\ldots,n$.
- $\hat{\lambda}_1 \times \cdots \times \hat{\lambda}_n = \det \boldsymbol{B}$ and thus, $\boldsymbol{B} \succeq \boldsymbol{0} \Rightarrow \det \boldsymbol{B} \geqslant 0$.

We then have

$$\boldsymbol{\Sigma} + \zeta \boldsymbol{I} \succeq \mathbf{0} \Rightarrow \det(\boldsymbol{\Sigma} + \zeta \boldsymbol{I}) = (\sigma_1 + \zeta)(\sigma_2 + \zeta)(\sigma_3 + \zeta) \geqslant 0 \tag{54}$$

with the solution

$$\zeta \geqslant -\sigma_3 \Longleftrightarrow -\sigma_3 + s = \zeta, \quad s \geqslant 0 \tag{55}$$

Similarly,

$$-\boldsymbol{\Sigma} + (k - a\zeta)\boldsymbol{I} \succeq \mathbf{0} \Rightarrow \det(-\boldsymbol{\Sigma} + (k - a\zeta)\boldsymbol{I}) = [-\sigma_1 + (k - a\zeta)][-\sigma_2 + (k - a\zeta)][-\sigma_3 + (k - a\zeta)] \tag{56}$$

so that

$$k - a\zeta \geqslant \sigma_1 \Longleftrightarrow \sigma_1 + z = k - a\zeta, \quad z \geqslant 0 \tag{57}$$

must hold. Combining (55) and (57) we have

$$\sigma_1 - a\sigma_3 + z + as = k, \quad s, z \geqslant 0 \tag{58}$$

or

$$\sigma_1 - a\sigma_3 \leqslant k \tag{59}$$

with equality only when $s = z = 0$, i.e., when both the constraints (52) and (53) are active.

References

Andersen, E.D., Roos, C., Terlaky, T., 2003. On implementing a primal-dual interior-point method for conic quadratic optimization. Mathematical Programming 95, 249–277.

Ben-Tal, A., Nemirovski, A., 2001. Lectures on Modern Convex Optimization: Analysis, Algorithms, and Engineering Applications. MPS-SIAM Series on Optimization.

Bisbos, C.D., Makrodimopoulos, A., Pardalos, P.M., 2005. Second–order cone programming approaches to static shakedown analysis in steel plasticity. Optimization Methods and Software 20, 25–52.

Borges, L.A., Zouain, N., Huespe, A.E., 1996. A nonlinear optimization procedure for limit analysis. European Journal of Mechanics, A/Solids 15 (3), 487–512.

Christiansen, E., Andersen, K.D., 1999. Computation of collapse loads with von Mises type yield condition. International Journal for Numerical Methods in Engineering 45, 1185–1202.

Colberg, P.C., 1998. The influence of the linearization of the yield surface on the load-bearing capacity of reinforced concrete slabs. Computer Methods in Applied Mechanics and Engineering 162, 351–358.

Fox, E.N., 1974. Limit analysis for plates: the exact solution for a clamped square plate of isotropic material obeying the square yield criterion and loaded by uniform pressure. Philosophical Transactions of the Royal Society A277, 121–155.

Gilbert, M., Tyas, A., 2003. Layout optimization of large-scale pin-jointed frames. Engineering Computations 8, 1044–1064.

Golub, G., van Loan, C., 1996. Matrix Computations. Johns Hopkins University Press.

Han, W., Reddy, B.D., 2001. Plasticity: The Variational Basis and Numerical Analysis. Springer-Verlag.

Johansen, K.W., 1943. Brudlinieteorier: Gjellerup, Copenhagen; 1943. English Translation: Yield-line Theory, Cement and Concrete Association, London.

Koiter, W.T., 1953. Stress–strain relations, uniqueness and variational theorems for elastic–plastic materials with a singular yield surface. Quarterly of Applied Mathematics 11, 350–354.

Krabbenhøft, K., Damkilde, L., 2002. Lower bound limit analysis of slabs with nonlinear yield criteria. Computers & Structures 80, 2043–2057.

Krabbenhøft, K., Damkilde, L., 2003. A general nonlinear optimization algorithm for lower bound limit analysis. International Journal for Numerical Methods in Engineering 56, 165–184.

Krabbenhøft, K., Lyamin, A.V., Sloan, S.W., Wriggers, P., in press. An interior-point algorithm for elastoplasticity, International Journal for Numerical Methods in Engineering.

Lyamin, A.V., Sloan, S.W., 2002a. Lower bound limit analysis using non-linear programming. International Journal for Numerical Methods in Engineering 55, 573–611.

Lyamin, A.V., Sloan, S.W., 2002b. Upper bound limit analysis using linear finite elements and non-linear programming. International Journal for Numerical and Analytical Methods in Geomechanics 26, 181–216.

Makrodimopoulos, A., 2006. Computational formulation of shakedown analysis as a conic quadratic optimization problem. Mechanics Research Communications 33, 72–83.

Makrodimopoulos, A., Martin, C.M., 2005a. A novel formulation of upper bound limit analysis as a second-order programming problem. In: Onate, E., Owen, D., (Eds.), Proc. Complas, Barcelona.

Makrodimopoulos, A., Martin, C.M., 2005b. Limit analysis using large-scale SOCP optimization. In: Proc. 13th Nat. Conf. of UK Association for Computational Mechanics in Engineering, Sheffield, pp. 21–24.

Martin, C.M., 2005. Exact bearing capacity calculations using the method of characteristics. In: Barla, G., Barla, M. (Eds.), Proc. IACMAG. Turin, pp. 441–450. See also: <http://www-civil.eng.ox.ac.uk/people/cmm/ncnqngamma.pdf>.

Moreau, J.J., 1963. Inf-convolution des fonctions numeriques sur un espace vectoriel proximite et dualite dans un espace hilbertien. Comptes Rendus de l'Academie des Sciences de Paris 256, 125–129.

Moreau, J.J., 1976. Application of convex analysis to the treatment of elastoplastic systems. In: Germain, P., Nayroles, B. (Eds.), Applications of Methods of Functional Analysis to Problems in Mechanics. Springer-Verlag, pp. 57–89.

Nash, S.G., Sofer, A., 1996. Linear and Nonlinear Programming. McGraw-Hill, New York, NY.

Nielsen, M.P., 1984. Limit Analysis and Concrete Plasticity. Prentice-Hall.

Pontes, I.D.S., Borges, L.A., Zouain, N., Lopes, F.R., 1997. An approach to limit analysis with cone-shaped yield surfaces. International Journal for Numerical Methods in Engineering 40, 4011–4032.

Reddy, B.D., Martin, J.B., 1994. Internal variable formulations of problems in elastostoplasticity: constitutive and algorithmic aspects. Applied Mechanics Reviews 47, 429–456.

Simo, J.C., 1998. Numerical analysis and simulation in plasticity. In: Ciarlet, P.G., Lions, J.L. (Eds.), Handbook of Numerical Analysis. Elsevier, pp. 179–499.

Sturm, J.F., 1999. SeDuMi 1.02, a MATLAB toolbox for optimizing over symmetric cones. Optimization Methods and Software 11–12, 625–653. Available from: <http://sedumi.mcmaster.ca/>.

Tutuncu, R.H., Toh, K.C., Todd, M.J., 2003. Solving semidefinite-quadratic linear programs using SDPT3. Mathematical Programming 95, 189–217. Available from: <http://www.math.nus.edu.sg/mattohkc/sdpt3.html>.

Vanderbei, R.J., 2001. Linear Programming: Foundations and Extensions. Springer-Verlag.

Wright, S.J., 1997. Primal-Dual Interior-Point Methods. SIAM, Philadelphia.

Yu, H.S., Sloan, S.W., Kleeman, P.W., 1994. A quadratic element for upper bound limit analysis. Engineering Computations 11, 195–212.

Zouain, N., Herskovits, J., Borges, L.A., Feijóo, R.A., 1993. An iterative algorithm for limit analysis with nonlinear yield functions. International Journal of Solids and Structures 30 (10), 1397–1417.